ORIGINAL PAPER

Biophysical Characterization of Bladder Cancer Cells with Different Metastatic Potential

Haijiao Liu · Qingyuan Tan · William R. Geddie · Michael A. S. Jewett · Nigel Phillips · Danbing Ke · Craig A. Simmons · Yu Sun

Abstract Specific membrane capacitance (SMC) and Young's modulus are two important parameters characterizing the biophysical properties of a cell. In this work, the SMC and Young's modulus of two cell lines, RT4 and T24, corresponding to well differentiated (low grade) and poorly differentiated (high grade) urothelial cell carcinoma (UCC), respectively, were quantified using microfluidic and AFM measurements. Quantitative differences in SMC and Young's modulus values of the high-grade and low-grade UCC cells are, for the first time, reported.

Keywords Bladder cancer cells · Specific membrane capacitance (SMC) · Young's modulus · Microfluidics · Atomic force microscopy (AFM)

Haijiao Liu and Qingyuan Tan contributed equally to this work.

H. Liu · Q. Tan · C. A. Simmons · Y. Sun (✉)
Department of Mechanical and Industrial Engineering,
University of Toronto, Toronto, ON M5S 3G8, Canada
e-mail: sun@mie.utoronto.ca

H. Liu · C. A. Simmons · Y. Sun
Institute of Biomaterials and Biomedical Engineering,
University of Toronto, Toronto, ON M5S 3G9, Canada

W. R. Geddie
Department of Laboratory Medicine and Pathobiology,
University of Toronto, Toronto, ON M5G 2C4, Canada

M. A. S. Jewett
Department of Surgical Oncology, Princess Margaret Hospital,
Toronto, ON M5G 2M9, Canada

N. Phillips · D. Ke
Bioniche Life Sciences Inc, Montreal, QC H4P 2R2, Canada

Introduction

It was estimated that over 141,140 people in the United States alone were diagnosed in 2012 with carcinoma of the urinary bladder [1]. Histopathologically, more than 90 % [1, 2] of bladder cancers are classified as urothelial (or "transitional") cell carcinomas (UCC or TCC). This carcinoma arises in cells lining the urinary bladder and has a propensity for recurrence, since the causative factors giving rise to urothelial carcinoma affect the entire urinary tract, an example of the so-called "field effect" [3].

T24, a cell line derived from poorly differentiated (grade III) bladder carcinoma [4], and RT4, derived from a grade I urothelial carcinoma (sometimes termed papilloma) [5], represent two extremes of the bladder carcinoma spectrum and have been extensively studied in bladder cancer research. These two cell lines are known to exhibit different human leukocyte antigen profiles [6], growth and migration characteristics [7], receptor expressions, morphological features [2, 8, 9], and in vitro responsiveness to chemotherapeutic agents, such as mitomycin C (MMC) [10]. However, the biophysical properties of these two bladder cancer cell lines are not known.

Biophysical properties of a cell include both electrical properties (e.g., cell membrane [11–13]) and mechanical properties [14]. Cell specific membrane capacitance (SMC), which is the membrane capacitance per unit surface area [13], is an electrical parameter that changes according to the cell's physiological state. It is known that for a smooth lipid bilayer membrane, the SMC value is in the range of 4–6 mF/m^2 [15]. Biological cells' SMC values are higher (e.g., 10–40 mF/m^2), since their membranes contain variable surface proteins and brush layers (microvilli, microridges, and cilia). Using atomic force microscopy (AFM) Iyer et al. [16] have shown that benign and

malignant epithelial cells have different membrane brush layers. Benign cells usually have a single-length brush layer, while cancerous cells have a brush layer with two characteristic lengths and higher grafting densities (number of 'molecules' per μm^2) than normal cells. Since RT4 and T24 are cancer cells of different grades, we hypothesized that their SMC values could have measurable differences.

Young's modulus, increasingly studied as a means of understanding cell phenotype, is associated with cell adhesion, invasion, and cytoskeletal organization [17, 18]. Cell stiffness has been used in several studies to identify cancerous cells, which show altered Young's modulus values compared to benign cells [19, 20]. Cancer progression is characterized by the disruption or reorganization of the cytoskeleton, which results in altered cancer cell stiffness and metastatic efficiency [21]. Thus, different Young's modulus values were expected in RT4 and T24 cells.

Materials and Methods

T24 and RT4 cells were purchased from the American Type Culture Collection (ATCC, Manassas, VA, USA). Cells were cultured in ATCC-formulated McCoy's 5a modified medium supplemented with 10 % fetal bovine serum and 1 % penicillin under 37 °C in a 100 % humidified 5 % CO_2 incubator.

Our microfluidic device for SMC measurements has been previously described [22]. For this study the device was modified to accommodate the sizes of RT4 and T24 cells. The device contains a tapered channel with entrance width 23.5 ± 0.4 μm, outlet width 8.02 ± 0.05 μm, channel length 118.2 ± 0.2 μm, and channel height 10.0 ± 0.5 μm ($n = 3$ chips). Cells were first trypsinized from the flask substrate. The cell suspension was mixed with fresh culture medium in 1:4 ratio. The cell suspension mixture was then added to the inlet reservoir of the device. Figure 1a–d show steps to trap a cell inside the tapered microfluidic channel. Electrodes were inserted into the inlet and outlet ports of the device for SMC measurement (Fig. 1e). During the SMC measurement, each cell's impedance profile was measured from 5 kHz to 1 MHz, including 201 measuring points that formed the cell's impedance spectrum. Detailed device operation and data processing methods were described elsewhere [22].

For mechanical characterization, RT4 and T24 cells were tested using an AFM (Bioscope Catalyst, Bruker, Santa Barbara, CA) mounted on an inverted optical microscope (Nikon Eclipse-Ti). The spherical tips were epoxy-glue assembled by manually attaching a borosilicate glass microsphere (radius = 4.870 μm) onto the cantilever right behind the standard pyramidal tip (MSCT-D, Bruker,

Santa Barbara, CA) (see Fig. 2a). Epoxy glue was completely cured before cell experiments to avoid potential toxicity effect on cells [23, 24], and only top half of the microsphere was bonded by epoxy glue to the cantilever.

For AFM measurements, RT4 and T24 cells were seeded at a density of 2,500 cells/cm^2 in a Petri dish. Cells were incubated at 37 °C with 5 % CO_2 for 24 h before performing AFM measurements. All measurements were made in the fluid environment at room temperature. All force curves were captured at four distinct spots on the cell surface with a height of at least 3 μm (i.e., on cell body)(Fig. 2b, c), and the trigger force applied to the cell was consistently 500 pN, to ensure that the indentation did not exceed 15 % of the height of the cell [25] and to avoid extraneous cantilever-cell contact [26] and substrate effect [27]. We repeated indentation at the same location of the cell five times and observed no significant change in the Young's moduli. The standard Hertz model was used to determine the cell's Young's modulus, as previously described [28]. Briefly, the Hertz model with Sneddon's modification, $F = \left(\frac{4}{3}\right)\sqrt{R}\left[\frac{E}{1-v^2}\right]h^{3/2}$ was applied to fit the approach trace of each force curve to estimate elastic modulus, where F is the loading force applied by the AFM, E is the Young's modulus of the sample, v is the Poisson ratio of the sample, h is the cell indentation depth, and R is the radius of the indenting sphere. The cantilever spring constants were calibrated every time before running the experiment by measuring the power spectral density of the thermal noise fluctuation of the unloaded cantilever [29].

For fluorescence imaging, RT4 and T24 cells were seeded in a 24-well plate at the same density as for AFM measurements, and were incubated for 24 h before staining. The cells were fixed with 10 % neutral buffered formalin, permeabilized with 0.1 % Triton X-100, and stained for F-actin (phalloidin, 1:25 dilution), followed by nuclear staining with Hoechst dye (1:500 dilution). Fluorescence images were taken using a fluorescence microscope (Olympus IX-71). The resulting images were analyzed using ImageJ. Multiple images were taken from distinct regions for each cell type and the total numbers of cells were counted, and a typical comparison is presented.

Both SMC and Young's modulus values are reported as mean ± standard error of the mean and were analyzed by one-way ANOVA for pairwise comparison. The statistical significance in each comparison was evaluated with $p \leq 0.05$ chosen to denote significance.

Results and Discussion

The average diameters of RT4 and T24 cells in their suspension state were measured to be 13.6 ± 1.3 μm ($n = 19$) and 13.1 ± 2.0 μm ($n = 20$). The SMC values of RT4 and
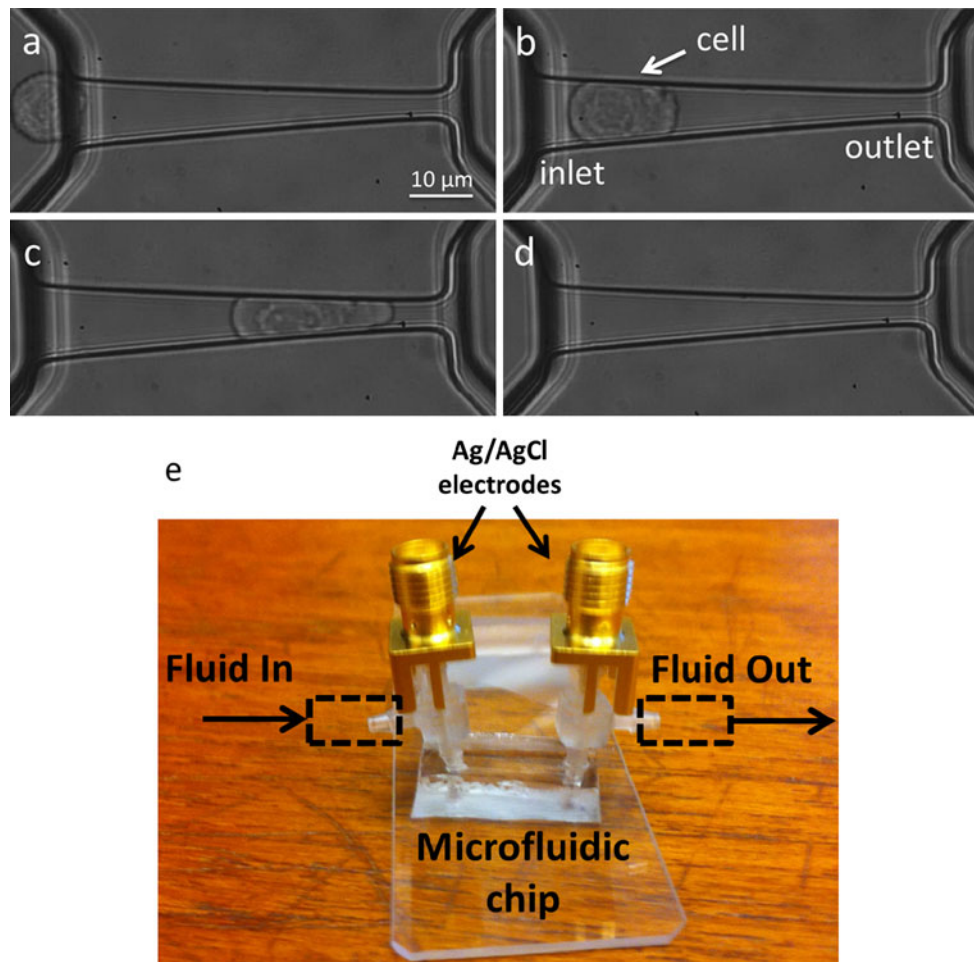
Fig. 1 a A T24 cell is first guided into the constriction channel via negative pressure. **b** Impedance measurements were conducted when the cell stops at a certain position inside the channel where suction force and friction force reach equilibrium. **c, d** The application of a larger suction force, after the impedance measurements, removes the cell out of the constriction channel. **e** Electrodes are inserted into the inlet and outlet ports of the device for electrical impedance measurement

T24 were measured to be 39.7 ± 8.3 mF/m^2 ($n = 19$) and 47.0 ± 5.1 mF/m^2 ($n = 20$), respectively (Fig. 3).

Electrically, the capacitance of the cell membrane is contributed by the lipid bilayer, associated proteins and other membrane structures [30]. RT4 cells and T24 cells are of different grades; however, they were derived from the same basic cell type [31]. Therefore, hydrocarbon molecule types which form the lipid bilayer of the two cell lines are not expected to differ significantly. As Wang et al. [30] reported, the capacitance contribution of the lipid bilayer is mainly determined by the non-polar hydrocarbon groups. Hence, the capacitance contribution of the lipid bilayer of RT4 cells and T24 cells could be considered similar.

The difference in SMC values of T24 cells and RT4 cells is likely due to their distinct membrane structures. It is known that T24 and RT4 cells have different membrane nanotubes densities [9, 31]. Membrane nanotubes grown on cell surface connect separate cells and offer an effective way for intercellular transport and communication. T24 cells are known to have denser nanotube structures than RT4 cells [9]. Thus, the total membrane surface area per patch of a T24 cell can be larger than the same sized RT4 cell patch. The extra surface area of the cell increases its charge storage ability, resulting in a higher capacitance value. Consequently, although the two cell lines have similar diameters, SMC values of T24 cells are significantly higher than RT4 cells ($p < 0.01$) likely due to their more complicated surface morphologies.

Mechanically, RT4 cells exhibit significantly ($p < 0.002$) higher Young's moduli (0.47 ± 0.04 kPa) than T24 cells (0.21 ± 0.02 kPa) (Fig. 4). The results reveal that T24, which is a high-grade invasive cell line, has reduced stiffness compared to RT4 (low-grade and non-invasive). The lower stiffness of high-grade cancer cells is in agreement with previously reported findings in
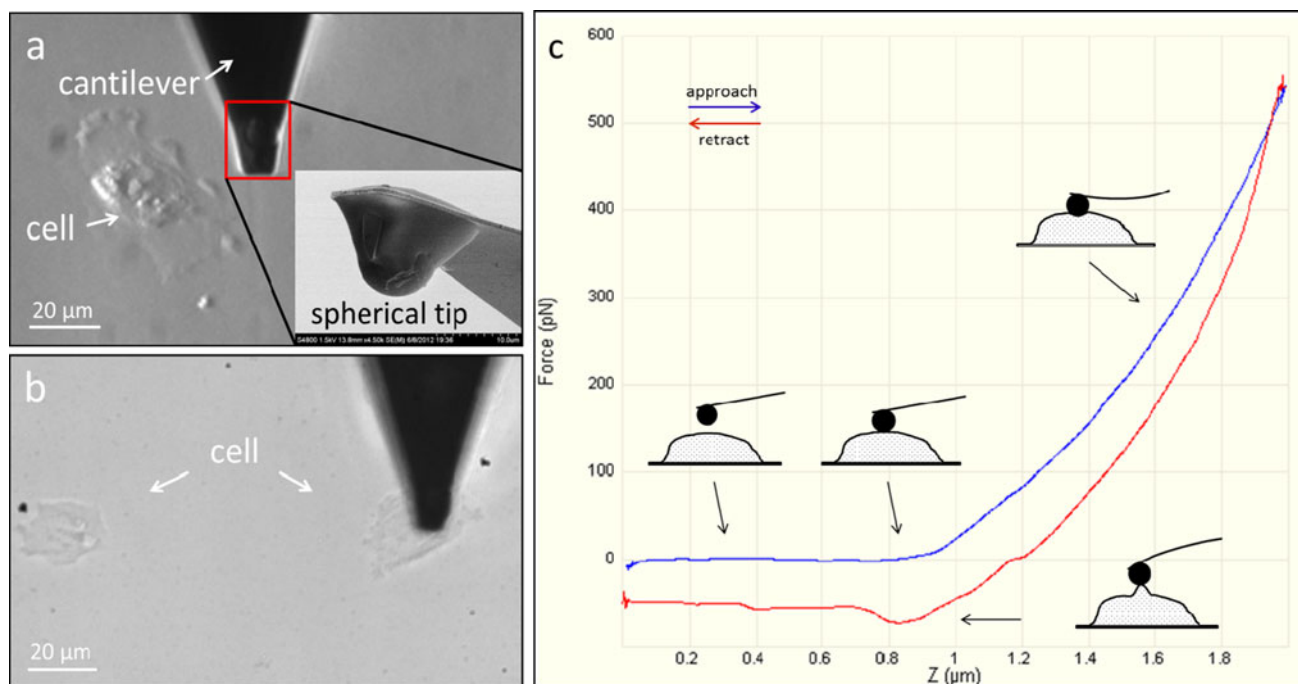
Fig. 2 **a** AFM indentation of a single cell. *Inset* shows a microsphere assembled onto a standard AFM tip. **b** AFM spherical tip in contact with cell. **c** A representative force–displacement curve with schematics showing each contact step with cell
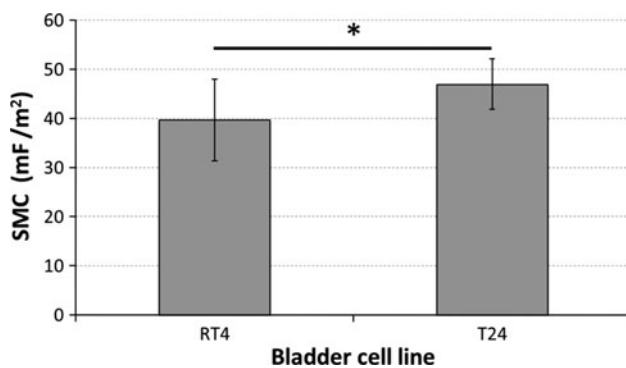

Fig. 3 Comparison of SMC values of RT4 ($n = 19$) and T24 cells ($n = 20$) (* $p < 0.01$)

Fig. 4 Comparison of the Young's modulus values of RT4 ($n = 39$) and T24 cells ($n = 14$) (* $p < 0.002$)

other cancer cells [14]. It is known that cancer cells differ from normal cells in many aspects, including cell metabolism [32], cell–cell interactions [33], and the organization of the cytoskeleton [34]. As cancer advances, cancerous cells show high activities of cell metabolism, and usually overexpress glycolytic enzymes [35]. Some of the glycolytic enzymes are associated with the cytoskeleton [36]. Importantly, the detachment of the cytoskeleton-associated enzymes from the cytoskeleton leads to a decrease in the glycolysis level, and also leads to the cell cytoskeleton reorganization by rearranging the actin network, since glycolytic enzymes were found to crosslink actin filaments into ordered structures [37]. Furthermore, the reorganization of the cell cytoskeleton causes changes in cell
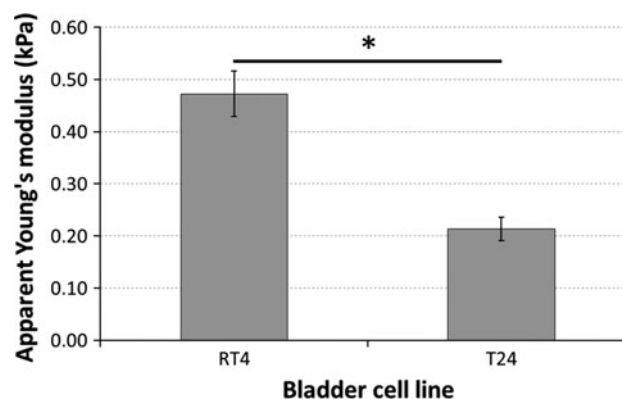
stiffness, since the mechanical response is primarily dominated by the actin filaments network directly beneath the cell membrane [38]. It has been shown that a low stiffness of breast cancer cells is accompanied by a partial loss of organized actin filaments and/or stress fibers, and therefore by a lower density of the cellular scaffold [39]. Studies of cell deformability confirmed that cancerous cells are less stiff than their normal counterpart cells [40]. Interestingly, it was also shown that T24 cells exhibited increased cell stiffness when the cellular glycolytic activity was strongly inhibited with the treatment of chitosan with high deacetylation degree, implying inhibition of enzymes bound to the cytoskeleton [41].
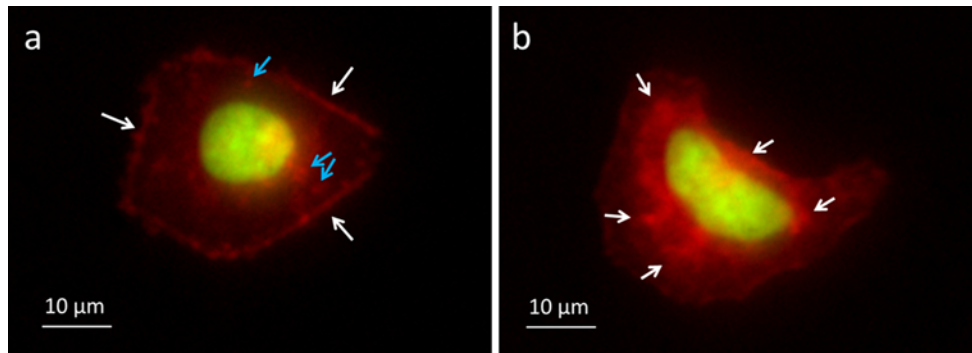
Fig. 5 Cytoskeletal F-actin (*red*) and nuclear staining (*green*) of **a** T24 cell and **b** RT4 cell. T24 cells (*n* = 126) have thin cortical actin filaments only (noted by *white arrows*) and show very few cytoplasmic actin. F-actin in T24 cells form a more disorganized network and appear to be fragmented into bright spots (noted by *blue arrows*). RT4 cells (*n* = 57) show higher cytoplasmic actin density (noted by *white arrows*) than T24 cells (Color figure online)

We further investigated the actin molecular structures in RT4 and T24 cells (see Fig. 5). The cells were F-actin labeled with phalloidin (red) and their nuclei labeled with Hoechst dye (green). Neither of the cells formed prominent actin stress fibers. RT4 cells (*n* = 57) show higher cytoplasmic actin density than T24 cells. In contrast, 82 % of T24 cells (*n* = 153 in total) have thin cortical actin filaments only and show very few cytoplasmic actin. F-actin in T24 cells form a more disorganized network and appear to be fragmented into bright spots. It has been shown that cell stiffness increases with cortical actin thickness, and that having only a thin cortical actin layer could result in soft and easily deformed cells [42, 43]. It has also been suggested that the cortical actin is softer than the "deeper" F-actin structure [44], which implies that the differences in stiffness between T24 and RT4 cells could be attributed to the differences in F-actin distribution (i.e., cortical vs. cytoplasmic). This may imply that the reorganized actin structure in T24 cell, possibly as a consequence of cancer progression, is one contributing factor to its lower stiffness.

Moreover, keratin intermediate filaments, which predominate in epithelial cells, could also contribute to lower stiffness of T24 cells via reorganizing their molecular network. It was shown that normal and cancerous cells express keratins differently in breast epithelial cells [45]. Treatment of human epithelial pancreatic cancer cells, with the naturally occurring bioactive lipid-SPC in concentrations comparable to that of malignant ascites in vivo, results in a threefold reduction in elastic stiffness as a result of reorganization of the keratin molecular network in the perinuclear region [46]. Similarly, differences in the expression of keratin intermediate filaments between RT4 and T24 cells could be expected. Further investigation is required to confirm its contribution to the measured cellular stiffness differences.

Conclusion

This study, for the first time, quantitatively demonstrated that bladder cancer cell lines of different grades possess different biophysical parameters (SMC and Young's modulus). Higher grade bladder cancer cells (T24) have larger SMC (47.0 ± 5.1 vs. 40.0 ± 8.3 mF/m^2) and lower Young's modulus (0.21 ± 0.02 vs. 0.47 ± 0.04 kPa) than the lower grade cells (RT4). These two bladder cancer cell lines are known to be different in chromosomal and morphological expression. The results from this study provide new knowledge about their biophysical properties and differences.

References

1. Siegel, R., Naishadham, D., & Jemal, A. (2012). Cancer statistics, 2012. *CA: A Cancer Journal for Clinicians, 62*, 10–29.
2. DeGraff, D. J., Clark, P. E., Cates, J. M., et al. (2012). Loss of the urothelial differentiation marker foxa1 is associated with high grade, late stage bladder cancer and increased tumor proliferation. *PLoS ONE, 2012*(7), e36669.
3. Jones, T. D., Wang, M., Eble, J. N., et al. (2005). Molecular evidence supporting field effect in urothelial carcinogenesis. *Clinical Cancer Research, 11*, 6512–6519.
4. Bubeník, J., Barešová, M., Viklický, V., et al. (1973). Established cell line of urinary bladder carcinoma (t24) containing tumour-specific antigen. *International Journal of Cancer, 11*, 765–773.
5. Franks, L., & Rigby, C. (1975). Letter: Hela cells and rt4 cells. *Science, 188*, 168.
6. O'Toole, C. M., Tiptaft, R. C., & Stevens, A. (1982). Hla antigen expression on urothelial cells: Detection by antibody-dependent cell-mediated cytotoxicity. *International Journal of Cancer, 29*, 391–395.
7. Kim, J., Ji, M., DiDonato, J., et al. (2011). An htert-immortalized human urothelial cell line that responds to anti-proliferative

factor. *In Vitro Cellular & Developmental Biology—Animal, 47*, 2–9.

8. Yamada, T., Ueda, T., Shibata, Y., et al. (2010). Trpv2 activation induces apoptotic cell death in human t24 bladder cancer cells: A potential therapeutic target for bladder cancer. *Urology, 76*, 509.

9. Lokar, M., Perutková, Š., Kralj-Iglič, V., et al. (2009). In A. L. Liu & I. Aleš (Eds.), *Advances in planar lipid bilayers and liposomes, vol. 10* (pp. 65–94). Burlington, ON: Academic Press.

10. van der Heijden, A. G., Jansen, C. F. J., Verhaegh, G., et al. (2004). The effect of hyperthermia on mitomycin-c induced cytotoxicity in four human bladder cancer cell lines. *European Urology, 46*, 670–674.

11. Bao, J. Z., Davis, C. C., & Schmukler, R. E. (1992). Frequency domain impedance measurements of erythrocytes. Constant phase angle impedance characteristics and a phase transition. *Biophysical Journal, 61*, 1427–1434.

12. Long, Q., & Xing, W. (2006). Detection of the apoptosis of jurkat cell using an electrorotation chip. *Frontiers of Biology in China, 1*, 208–212.

13. Arnold, W. M., & Zimmermann, U. (1982). Rotating-field-induced rotation and measurement of the membrane capacitance of single mesophyll-cells of avena-sativa. *Zeitschrift Fur Naturforschung Section C: A Journal of Biosciences., 37*, 908–915.

14. Cross, S. E., Jin, Y.-S., Rao, J., et al. (2007). Nanomechanical analysis of cells from cancer patients. *Nat Nano., 2*, 780–783.

15. Gross, L. C. M., Heron, A. J., Baca, S. C., et al. (2011). Determining membrane capacitance by dynamic control of droplet interface bilayer area. *Langmuir, 27*, 14335–14342.

16. Iyer, S., Gaikwad, R. M., Subba Rao, V., et al. (2009). Atomic force microscopy detects differences in the surface brush of normal and cancerous cells. *Nature Nanotechnology, 2009*(4), 389–393.

17. Discher, D. E., Janmey, P., & Wang, Y.-L. (2005). Tissue cells feel and respond to the stiffness of their substrate. *Science, 310*, 1139–1143.

18. Rotsch, C., & Radmacher, M. (2000). Drug-induced changes of cytoskeletal structure and mechanics in fibroblasts: An atomic force microscopy study. *Biophysical Journal, 78*, 520–535.

19. Guck, J., Schinkinger, S., Lincoln, B., et al. (2005). Optical deformability as an inherent cell marker for testing malignant transformation and metastatic competence. *Biophysical Journal, 88*, 3689–3698.

20. Suresh, S., Spatz, J., Mills, J. P., et al. (2005). Connections between single-cell biomechanics and human disease states: Gastrointestinal cancer and malaria. *Acta Biomaterialia, 1*, 15–30.

21. Yamaguchi, H., & Condeelis, J. (2007). Regulation of the actin cytoskeleton in cancer cell migration and invasion. *Biochimica et Biophysica Acta, 1773*, 642–652.

22. Tan, Q. Y., Ferrier, G. A., Chen, B. K., et al. (2012). Quantification of the specific membrane capacitance of single cells using a microfluidic device and impedance spectroscopy measurement. *Biomicrofluidics, 2012*, 6.

23. Kydd, W. L. (1960). Toxicity evaluation of diethylenetriamine. *Journal of Dental Research, 39*, 46–48.

24. Kapsimalis, P. (1960). Toxicity studies of cured epoxy resins. *Journal of Dental Research, 39*, 1072.

25. Costa, K. D., & Yin, F. C. (1999). Analysis of indentation: Implications for measuring mechanical properties with atomic force microscopy. *Journal of Biomechanical Engineering, 121*, 462–471.

26. Harris, A. R., & Charras, G. T. (2011). Experimental validation of atomic force microscopy-based cell elasticity measurements. *Nanotechnology, 2011*(22), 345102.

27. Akhremitchev, B. B., & Walker, G. C. (1999). Finite sample thickness effects on elasticity determination using atomic force microscopy. *Langmuir, 15*, 5630–5634.

28. Liu, H. J., Sun, Y., & Simmons, C. A. (2013). Determination of local and global elastic moduli of valve interstitial cells cultured on soft substrates. *Journal of Biomechanics*. doi:10.1016/j.jbiomech.2013.05.001.

29. Ohler, B. (2007). Cantilever spring constant calibration using laser Doppler vibrometry. *Review of Scientific Instruments, 2007*(78), 063701.

30. Wang, X.-B., Huang, Y., Gascoyne, P. R. C., et al. (1994). Changes in friend murine erythroleukaemia cell membranes during induced differentiation determined by electrorotation. *Biochimica et Biophysica Acta, 1193*, 330–344.

31. Kabaso, D., Lokar, M., Kralj-Iglič, V., et al. (2011). Temperature and cholera toxin b are factors that influence formation of membrane nanotubes in rt4 and t24 urothelial cancer cell lines. *International Journal of Nanomedicine, 6*, 495–509.

32. Mazurek, S., Grimm, H., Wilker, S., et al. (1998). Metabolic characteristics of different malignant cancer cell lines. *Anticancer Research, 18*, 3275–3282.

33. Ben-Ze'ev, A. (1997). Cytoskeletal and adhesion proteins as tumor suppressors. *Current Opinion in Cell Biology, 9*, 99–108.

34. Rao, K. M. K., & Cohen, H. J. (1991). Actin cytoskeletal network in aging and cancer. *Mutation Research/DNAging, 256*, 139–148.

35. Gumińska, M., Ignacak, J., Kedryna, T., et al. (1997). Tumor-specific pyruvate kinase isoenzyme m2 involved in biochemical strategy of energy generation in neoplastic cells. *Acta Biochimica Polonica, 44*, 711–724.

36. Janmey, P. A. (1998). The cytoskeleton and cell signaling: Component localization and mechanical coupling. *Physiological Reviews, 78*, 763–781.

37. Glass-Marmor, L., & Beitner, R. (1997). Detachment of glycolytic enzymes from cytoskeleton of melanoma cells induced by calmodulin antagonists. *European Journal of Pharmacology, 328*, 241–248.

38. Tsai, M. A., Waugh, R. E., & Keng, P. C. (1998). Passive mechanical behavior of human neutrophils: Effects of colchicine and paclitaxel. *Biophysical Journal, 74*, 3282–3291.

39. Li, Q. S., Lee, G. Y. H., Ong, C. N., et al. (2008). Afm indentation study of breast cancer cells. *Biochemical and Biophysical Research Communications, 374*, 609–613.

40. Lekka, M., Laidler, P., Gil, D., et al. (1999). Elasticity of normal and cancerous human bladder cells studied by scanning force microscopy. *European Biophysics Journal, 28*, 312–316.

41. Lekka, M., Laidler, P., Ignacak, J., et al. (2001). The effect of chitosan on stiffness and glycolytic activity of human bladder cells. *Biochimica et Biophysica Acta, 1540*, 127–136.

42. MacQueen, L. A., Thibault, M., Buschmann, M. D., et al. (2012). Electromechanical deformation of mammalian cells in suspension depends on their cortical actin thicknesses. *Journal of Biomechanics, 45*, 2797–2803.

43. Ananthakrishnan, R., Guck, J., Wottawah, F., et al. (2006). Quantifying the contribution of actin networks to the elastic strength of fibroblasts. *Journal of Theoretical Biology, 242*, 502–516.

44. Laurent, V. M., Fodil, R., Canadas, P., et al. (2003). Partitioning of cortical and deep cytoskeleton responses from transient magnetic bead twisting. *Annals of Biomedical Engineering, 31*, 1263–1278.

45. Trask, D. K., Band, V., Zajchowski, D. A., et al. (1990). Keratins as markers that distinguish normal and tumor-derived mammary epithelial cells. *Proceedings of the National Academy of Sciences, 87*, 2319–2323.

46. Beil, M., Micoulet, A., von Wichert, G., et al. (2003). Sphingosylphosphorylcholine regulates keratin network architecture and visco-elastic properties of human cancer cells. *Nature Cell Biology, 5*, 803–811.